Digital Tracking Array Using Off-the-Shelf Hardware

Levent Gezer, Robert Broadston, David Jenn and Gert Burgstaller

Naval Postgraduate School
833 Dyer Road, Room 437
Monterey, CA, 93943 USA
Tel: +1 (831) 656-2254; E-mail: jenn@nps.edu

Abstract

The design, development, and testing of a digital tracking array is described. The array operates at 2.4 GHz for tracking video and data from UAVs and other mobile transmitters. A monopulse tracking technique is used to keep the beam scanned to the direction of the incoming signal. The array is built entirely of commercial off-the-shelf (COTS) components. Calibration, measurement of patterns, and verification of the tracking function are also discussed.

Keywords: Antenna arrays; tracking; monopulse antenna; array signal processing; demodulation

1. Introduction

Digital beamforming has many advantages over conventional beamforming [1, 2]. A digital antenna provides complete control of the amplitude and phase at every element, allowing the potential to provide a wide variety of desirable pattern features that can be changed dynamically by software. These include rapid beam scanning and accurate beam pointing, pattern shaping by precise amplitude and phase control, and multiple beams. Digital architecture allows flexibility in processing and array reconfiguration for multiple functions.

With the growth in wireless devices over the last ten years, many of the critical components required for digital arrays, such as the modulators and demodulators, have become widely available at low cost. This article describes the design and development of a digital array to receive and track signals from unmanned air vehicles (UAVs) and mobile transmitters. The array uses an error signal from the difference beam to correct beam-pointing errors and to continuously scan the sum beam in the direction of the incoming signal, as illustrated in Figure 1.

Analog Devices (AD) AD8347 quadrature demodulators are used to directly down-convert the signal at each element. National Instruments (NI) Compact Realtime I/O (cRIO) controllers and modules perform the data collection and transfer to a host computer, where the beam is formed in the processor.

2. Array Design

The array operates at $f = 2.4\,\text{GHz}$ so that it can track video and data signals from the UAV transmitted at that frequency. An array beamwidth in the range of 10° to 20°, with a maximum scan of ±40° from broadside, was deemed acceptable for the given operational ranges and velocities of the UAVs [3]. The array is comprised of eight elements, equally spaced at $d = 6.5\,\text{cm}$ (0.52 wavelength) to assure that no grating lobes occur at the maximum scan [4]. The antenna elements are printed-circuit dipoles above a finite ground plane [5]. A *Microwave Studio* [6] model of the complete array is shown in Figure 2. The simulated broadside sum and difference beams are shown in Figure 3. The difference beam is formed by subtracting the outputs from the left half of the array (elements 1 through 4) from those of the right half (elements 5 through 8). The algorithm for beamforming is discussed in Section 3.

A block diagram of the array's architecture is shown in Figure 4. A low-noise amplifier (LNA) is located at the output of each element. The output of the low-noise amplifier is fed to the RF input of an AD8347 quadrature demodulator. An AD8347 evaluation board is shown in Figure 5, and its specifications can be found in [7]. It operates from 800 to 2700 MHz with a modulation bandwidth of about 50 MHz.

For a signal at carrier frequency f, with amplitude A and phase Φ,

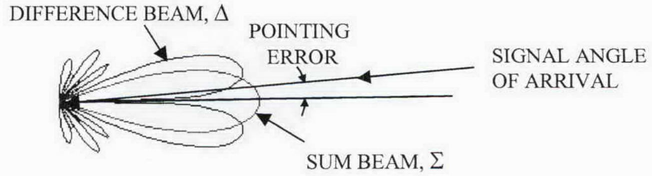

Figure 1. The sum and difference beams used for antenna pointing.

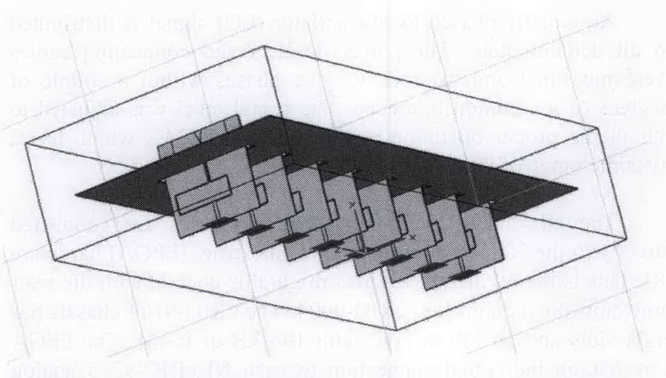

Figure 2. A *Microwave Studio* model of the array and ground plane (viewed from the back of the ground plane).

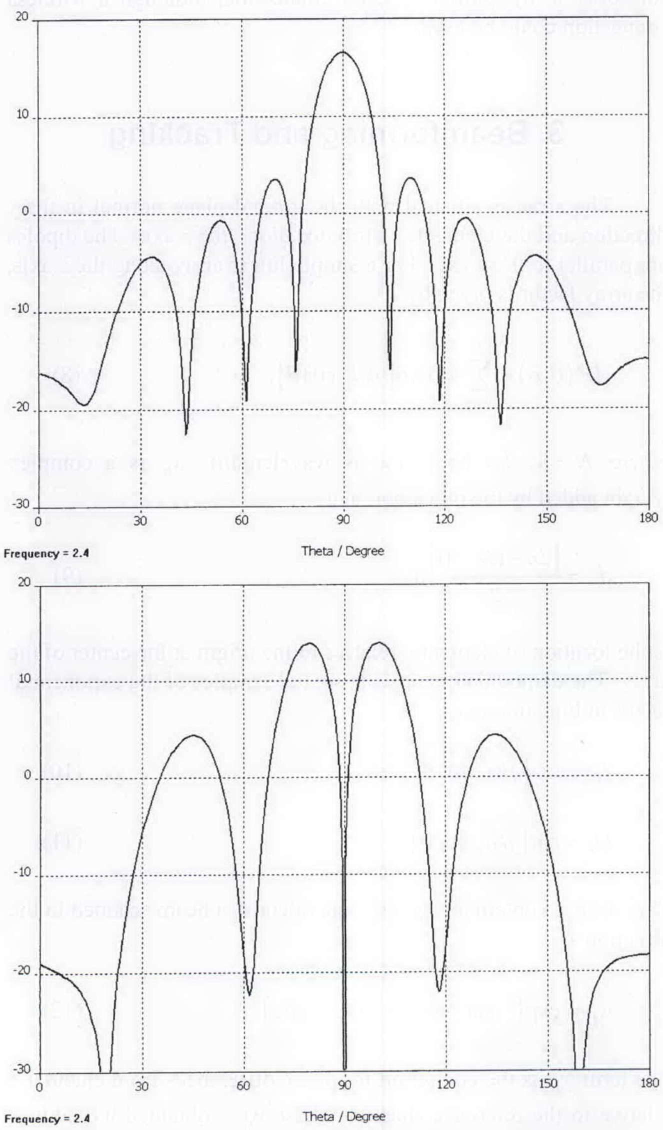

Figure 3. The computed sum and difference patterns for the array at broadside scan.

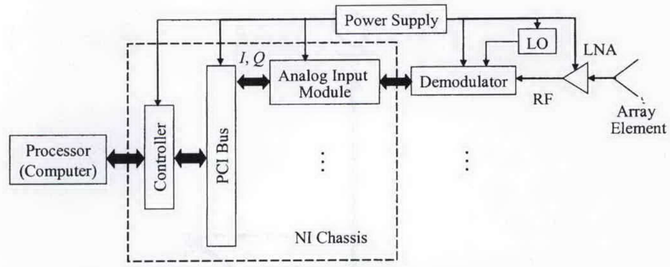

Figure 4. The array architecture (only one channel is shown).

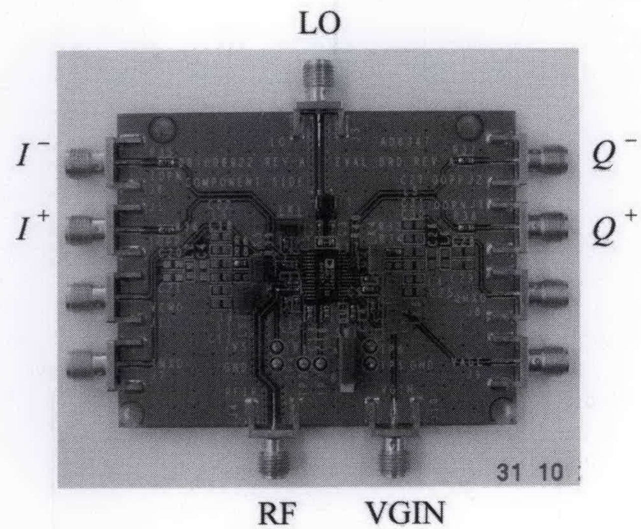

Figure 5. The Analog Devices AD8347 evaluation board.

$$s(t) = A(t)\cos\left[2\pi f t + \Phi(t)\right]. \quad (1)$$

The in-phase (I) and quadrature (Q) representation is given by

$$s(t) = I(t)\cos(2\pi f t) - Q(t)\sin(2\pi f t), \quad (2)$$

where

$$I(t) = A(t)\cos\left[\Phi(t)\right], \quad (3)$$

$$Q(t) = A(t)\sin\left[\Phi(t)\right]. \quad (4)$$

The amplitude and phase represents a point on the I, Q plane, as shown in Figure 6. The phase is obtained from the quadrature components by

$$\Phi(t) = \tan^{-1}\left[Q(t)/I(t)\right]. \quad (5)$$

The demodulator has differential outputs (I^+, I^-, Q^+, and Q^-) for obtaining the baseband in-phase and quadrature components of the received signal. The components are given by

$$I = I^+ - I^-, \quad (6)$$

$$Q = Q^+ - Q^-. \quad (7)$$

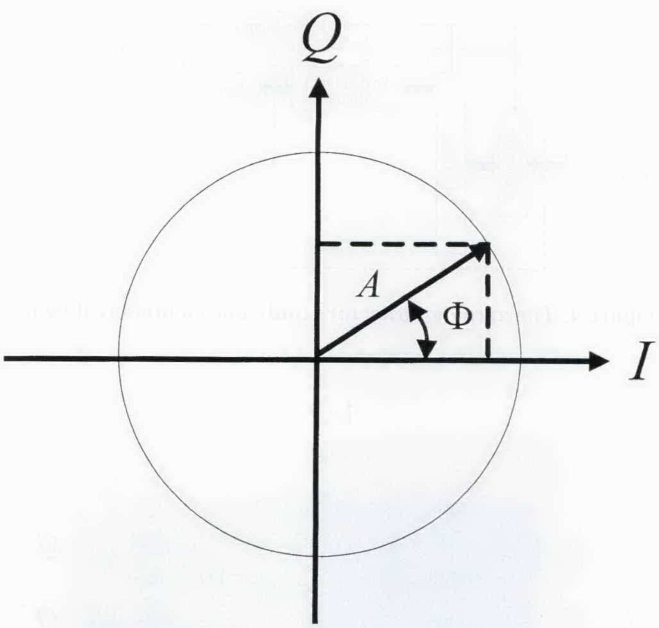

Figure 6. The in-phase and quadrature plane.

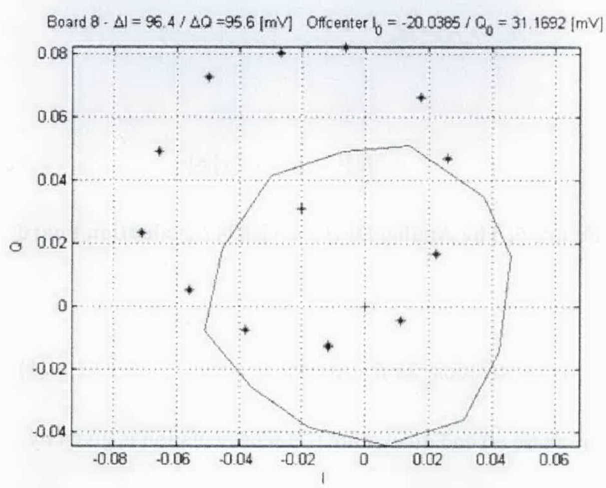

Figure 7. The measured phase data for a typical demodulator board (*) and with the offset removed (solid line).

In the process of characterizing the demodulators, it was found that the *I*/*Q* circles were not centered, and that each board had a unique offset. Therefore, it was necessary to calibrate every board and to correct for the offsets in the beam processing. Mechanically adjustable phase shifters were used to introduce phase shifts from 0° to 360°. The phase obtained from the measured *I*/*Q* components is plotted in Figure 7 for a typical demodulator. The radius of the circle is determined by the voltage, VGIN, which controls the baseband amplification. The NI9215 analog input module, which follows the demodulators, has 16-bit resolution, but a fixed ±10 V input range. Therefore, larger circles are preferred because they give smaller quantization errors. Typical voltage ranges for the AD8347 were 1±0.05 V, i.e., the *I*/*Q* circle radius was about 100 mV. After sampling, the voltage quantization step is approximately 0.305 mV. Each AI module has four channels, so one module is required to sample the four differential voltages from each demodulator.

An equally phased local-oscillator (LO) signal is distributed to all demodulators. The power dividers and connecting cables were measured and trimmed to give phases within a couple of degrees of a common reference. The signal level was adjusted to fall in the proper operating range for the AD8347, which has a dynamic range of 80 dB [3].

The NI cRIO-9215 analog input modules are connected directly to the NI field-programmable gate array (FPGA) hardware [8]. This is the NI cRIO-9104 reconfigurable chassis with the real-time embedded controller, cRIO-9004. The cRIO-9104 chassis has eight slots and an FPGA core with 196 kB of RAM. The FPGA core has an individual connection to each NI cRIO-9215 analog input module, and can read information from all modules simultaneously at a rate of 100 kS/s. The FPGA circuitry in the cRIO-9104 chassis passes the data to the real-time embedded controller through a local PCI bus. The cRIO-9004 includes 64 MB of DRAM memory and 512 MB of nonvolatile flash storage for data-logging applications. Embedded software code processes the data from the I/O modules and transfers the data to the host program, running *LabView* software [9]. This FPGA program is synchronized with the host program on a laptop computer by the means of an FPGA-generated interrupt request (IRQ) or an internal millisecond real-time clock source. Communication between the host and controller is by hardwired LAN connection, although a wireless connection could be used.

3. Beamforming and Tracking

The array is situated with the ground plane normal in the *y* direction and the elements distributed along the *z* axis. The dipoles are parallel to the *x* axis. For a simple linear array along the *z* axis, the array factor is given by

$$AF(\theta,\phi) = \sum_{n=1}^{N} w_n \exp\left[jkd_n \cos\theta\right], \tag{8}$$

where $N = 8$, $k = 2\pi/\lambda$ (λ is wavelength), w_n is a complex weight added by the processor, and

$$d_n = \frac{\left[2n-(N+1)\right]}{2} d \tag{9}$$

is the location of element *n* relative to the origin at the center of the array. The demodulators provide spatial samples of the exponential factor in Equation (8):

$$I_n = \cos\left[jkd_n \cos\theta\right], \tag{10}$$

$$Q_n = \sin\left[jkd_n \cos\theta\right]. \tag{11}$$

Therefore, to obtain a response equivalent to a beam scanned in the direction θ_s,

$$w_n = \exp\left[-jkd_n \cos\theta_s + j\gamma_n + j\psi_n\right]. \tag{12}$$

The term γ_n is the correction for phase differences from channel *n* relative to the reference channel. These were obtained by calibration. The ψ_n are zero for the sum beam; for the difference beam, half are zero ($N/2 < n \le N$) and half are π ($1 \le n \le N/2$).

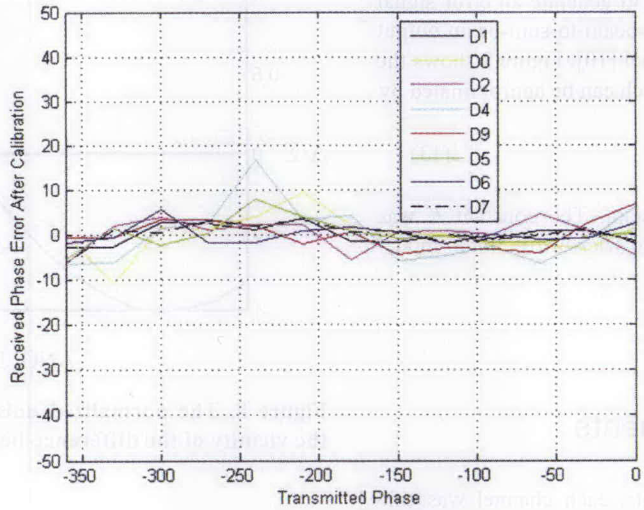

Figure 9. The measured phase as a function of the transmitted phase for the eight channels after calibration.

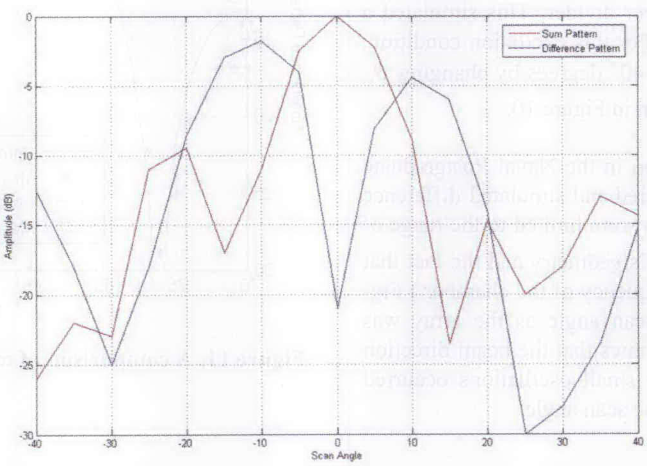

Figure 10. The bench-top scan pattern for broadside incidence.

A monopulse technique was used to generate an error signal for tracking. The ratio of the difference-beam-to-sum-beam output is generally used to derive the error signal [10]. Figure 8 shows the ratio Δ/Σ in the vicinity of the null, which can be approximated by

$$\Delta/\Sigma \approx K\theta . \quad (13)$$

where K is the monopulse slope constant. The constant K was obtained for various scan angles from the *Microwave Studio* model shown in Figure 2.

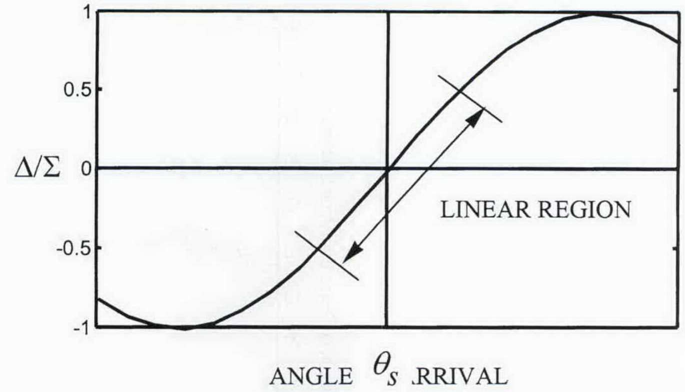

Figure 8. The normalized noiseless sum-to-difference ratio in the vicinity of the difference-beam null.

4. Measurements

After assembly of the components, each channel was calibrated by cycling an input signal through 360° and measuring the received phase using the *I* and *Q* outputs. The *I*/*Q* circle offsets and any constant phase shift between channels was calculated. The corrected data for the eight channels are presented in Figure 9. This plot characterizes the phase-measurement capability of the array; the residual errors shown are not be removed by processing.

A bench-top check of the array scanning was performed by disconnecting the dipoles and feeding the amplifiers directly with an RF signal split through a 1:8 power divider. This simulated a plane wave incident from broadside. For this excitation condition, the beam was scanned from −40° to 40° degrees by changing θ_s in Equation (12). The results are shown in Figure 10.

Pattern measurements were taken in the Naval Postgraduate School anechoic chamber. The measured and simulated difference patterns are shown in Figure 11. (Data were limited to the range of $\pm 20^\circ$ degrees because of the chamber's geometry and the fact that this frequency is below the design frequency of the chamber.) Figure 12 is a time strip chart of the scan angle as the array was rotated at a constant rate. The chart shows that the beam direction remained pointed at the source. The small oscillations occurred because of slight over-corrections in the scan angle.

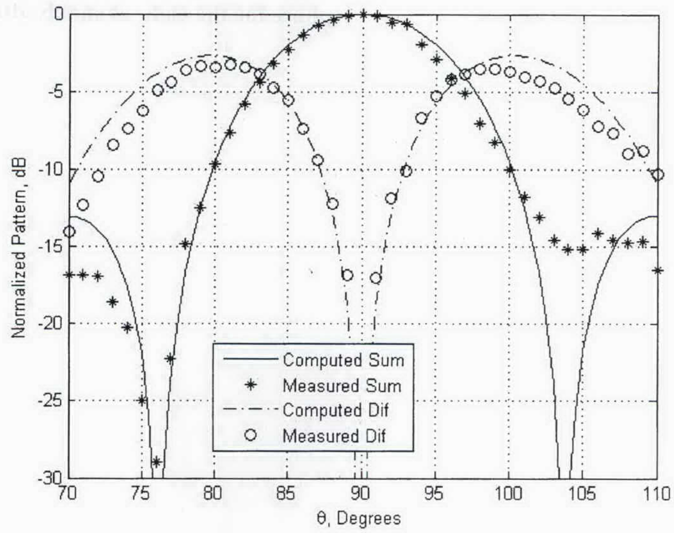

Figure 11. A comparison of measured and simulated patterns.

5. Summary and Conclusions

A digital tracking array, employing commercial off-the-shelf components, was designed, simulated in *Microwave Studio*, and subsequently built and tested. Before construction of the array, the devices were characterized using a vector network analyzer. The demodulator boards were found to have individual offsets that needed to be corrected in the beam processing. The final results were in good agreement with measured data, and tracking was demonstrated in an anechoic chamber by rotating the array and verifying that the beam remained pointed at the transmitting antenna. The total cost of the antenna was less than US$10,000, not including the software licenses and laptop computer.

Field testing of the array is planned, and upgrading the design to include a transmitting function is also in progress. Similar to the receiving side, the transmitting channels will utilize commercially available modulator boards (AD8346) and analog output modules (NI cRIO 9263).

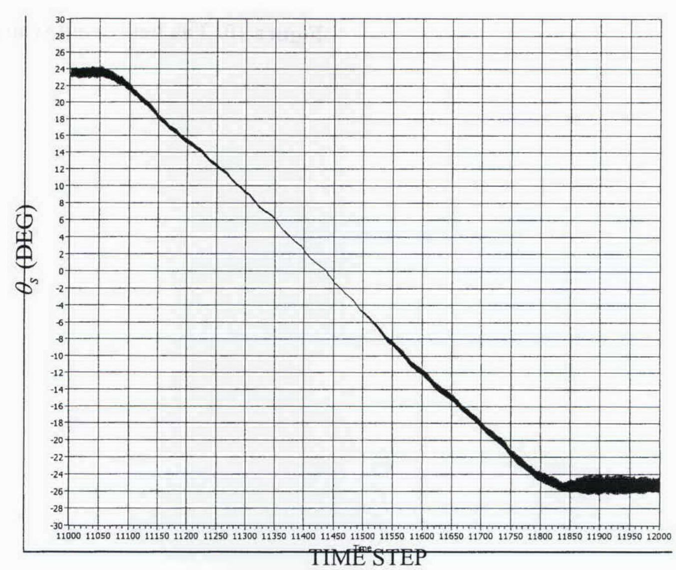

Figure 12. A time strip chart showing the beam scan angle as the array was rotated from 25° to −25° (0° was broadside).

6. References

1. J. Litva, *Digital Beamforming in Wireless Communications*, Norwood, MA, Artech House.

2. H. Steyskal, "Digital Beamforming Antennas: An Introduction," *Microwave Journal*, **30**, 1, January 1987, pp. 107-124.

3. L. Gezer, "Multi-Beam Digital Antenna for Radar, Communications, and UAV Tracking Based on Off-the-Shelf Wireless Technologies," Masters Thesis, Naval Postgraduate School, Monterey, CA, September 2006.

4. W. Stutzman and G. Thiele, *Antenna Theory and Design, Second Edition*, New York, Wiley, 1998.

5. R. S. Chu and K. M. Lee, "Radiation Impedance of Dipole Printed on Periodic Dielectric Slabs Protruding Over a Ground Plane and in an Infinite Phased Array," *IEEE Transactions on Antennas and Propagation*, **AP-35**, 1, January 1987, pp. 13-25.

6. CST Microwave Studio, January 2007, http://www.cst.com/Content/Products/MWS/Overview.aspx.

7. Analog Devices AD8347 Quadrature Demodulator, October 2005, http://www.analog.com/UploadedFiles/Data_Sheets/230407246AD8347_a.pdf.

8. National Instruments, "NI CompactRIO – Reconfigurable Control and Acquisition System," http://www.ni.com/compactrio/whatis.htm, retrieved February 2006.

9. National Instruments, "What is LabView?" http://www.ni.com/labview/whatis, retrieved August 2006.

10. N. Levanon, *Radar Principles*, New York, Wiley-Interscience, 1988.

Introducing the Feature Article Authors

Levent Gezer was born in Istanbul, Turkey, on July 20, 1978. He received the BS degree in Electrical Engineering from the Turkish Naval Academy in August 2000 in Communications.

From September 2000 to August 2004 he worked on radar, electronic warfare, and communication systems in the Turkish Navy as an Electronic Maintenance Officer and Electronic Warfare Officer. He received an MS degree in Systems Engineering from the Naval Postgraduate School, Monterey, CA, USA in September 2006. During his graduate education, he focused his studies on radar and electronic warfare systems. He designed and developed a digital phased-array tracking system.

Levent Gezer is currently working on a sensor and communications networking project (Integrated Maritime Surveillance System) for the Turkish Navy as a systems and test engineer.

Robert D. Broadston received the BSEE from the United States Naval Academy in 1984, and the MSEE and Electrical Engineer degrees from the United States Naval Postgraduate School in 2000. From 1984 to 2002, he served in the US Navy as a Naval aviator. From 2002-2004, he served as military faculty at the Naval Postgraduate School. Since 2004, he has been the Laboratory Director for the ECE Department's Microwave, Networking, and Digital Signal Processing Labs at the Naval Postgraduate School. He is currently pursuing a PhD in Electrical Engineering.

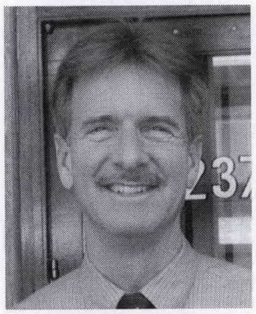

David C. Jenn received the PhD degree in Electrical Engineering from the University of Southern California in 1987. From 1976 to 1978, he was with McDonnell Douglas Astronautics Co., where he was involved in the design of small arrays and radomes for spacecraft and airborne platforms. In 1978, he joined Hughes Aircraft Co., where he concentrated on the design and analysis of high-performance phased-array antennas for radar and communication systems, and radar cross section analysis. During this time, Dr. Jenn contributed to the development of the AN/TPQ-37 Firefinder radar, and the Hughes Air Defense Radar (HADR).

In 1990, he joined the Department of Electrical and Computer Engineering at the Naval Postgraduate School, where he is currently a Professor. His research has covered a wide range of topics in electromagnetics, including microwave circuits and devices, antennas, and scattering and propagation. Prof. Jenn has also studied the effects of complex scattering environments – such as urban areas, aircraft, and ships – on the performance of radar and communication systems. Recent research has focused on integrated digital antennas for radar, communication, and electronic warfare applications.

While at NPS, Prof. Jenn has taught courses in the areas of antennas, propagation, radar, radar cross section, electromagnetic theory, and telecommunications. He has advised more than 80 masters-thesis students from the US and over 20 other countries. Prof. Jenn is Faculty Director of the NPS Microwave and Antenna Laboratory and author of the book *Radar and Laser Cross Section*

Engineering. He is a Senior Member of the IEEE, the American Institute of Aeronautics and Astronautics (AIAA), Tau Beta Pi, American Society for Engineering Education (ASEE), the Society of Optical Engineers (SPIE), and the Applied Computational Electromagnetics Society (ACES). A short list of publications and description of selected research projects are available on the Web at http://www.nps.navy.mil/facutly/jenn.

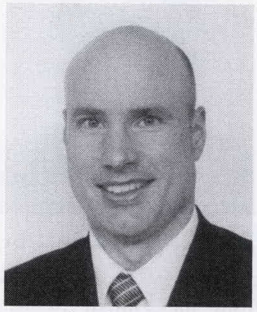

Gert Burgstaller received an MS degree in Electrical Engineering in 1996 from Chalmers University of Technology in Gothenburg, Sweden. After a second academic period, he added the Electrical Engineer's degree, combined with another MS EE degree in 2006 from the Naval Postgraduate School, Monterey, CA. He concluded the studies for the first MS EE degree with a year at the Technische Universität in München (TUM), Germany, as a holder of an ERASMUS scholarship. The associated research was partly sponsored by a LEONARDO scholarship, and was conducted at the Siemens Corporate Technology and Development department in Neuperlach Süd, Munich, Germany. For the EE degree, his research contributed to the development of a distributed phased array for radar and communications that incorporates wireless beamforming.

He is an active duty Naval officer in the Swedish Armed Forces, and currently carries the rank Commander (Engineer). Between the two academic periods, CDR Burgstaller held various engineers' positions within the Swedish Armed Forces and the Swedish Defense Material Administration (FMV), where the emphasis has been on sensor evaluation and sea trials of the stealthy VISBY class corvettes. Presently, he serves as the Chief of Joint Telecom Branch at the Swedish Joint Head Quarters in Stockholm.

IEEE China Office Inaugurated

The official inauguration of the IEEE China office in Beijing took place in Beijing January 21, 2008, with more than 150 representatives from industry, academia, government, and the IEEE in attendance. Those attending the ceremony included:

- Shang Yong, Vice Minister, Ministry of Science and Technology
- Yanchang Lu, vice president of the China Association for Science and Technology
- Wu Hequan, Vice President, Chinese Academy of Engineering
- Yaqin Zhang, Corporate Vice President, Microsoft (IEEE Fellow)
- Kai-Fu Lee, Vice President, Google (IEEE Fellow)

Lew Terman, 2008 IEEE President, delivered opening remarks to the attendees, who included IEEE Section Chairs and representatives from Beijing, Shanghai, Xi'an, Harbin, Chengdu, Wuhan, and Nanjing, as well as former Region 10 Director Seiichi Takeuchi. "It is our hope that through our presence here we will enhance the visibility of IEEE members in China as they link more easily to the global technical community," Terman said.

[The above item was taken from *IEEE Leadership Wire*.]